Nanoparticle Effect on the Dynamics of Polymer Chains and Their Entanglement Network

Ying Li, Martin Kröger, and Wing Kam Liu

Nanoparticle effect on the dynamics of polymer chains and their entanglement network

Ying Li,[1] Martin Kröger,[2] and Wing Kam Liu[1, 3, *]

[1]*Department of Mechanical Engineering, Northwestern University, 2145 Sheridan Road, Evanston, IL 60208-0311, USA*
[2]*Polymer Physics, Department of Materials, ETH Zurich, CH–8093 Zurich, Switzerland*
[3]*Visiting Distinguished Chair Professor, School of Mechanical Engineering,*
World Class University (WCU) Program in Sungkyunkwan University, Korea

We explore the dynamics of entangled polymer chains embedded into nanocomposites. From primitive path analysis, highly entangled polymer chains are found to be significantly disentangled during increment of the volume fraction of spherical non-attractive nanoparticles (NPs) from 0 to 42%. A critical volume fraction, $\phi_c = 31\%$, is found to control the crossover from polymer chain entanglements to 'NP entanglements'. While below ϕ_c, the polymer chain relaxation accelerates upon filling, above ϕ_c, the situation reverses: Polymer dynamics becomes geometrically constrained upon adding NPs. Our findings provide a microscopic understanding of the dynamics of entangled polymer chains inside their composites, and they offer an explanation for the unusual rheological properties of polymer composites.

In polymer nanocomposites (PNCs), fillers with dimensions on the nanometer scale added into polymers offer a huge enhancement on the mechano–viscoelastic properties of polymers. Understanding the nanoparticle (NP) effect on the polymer chain dynamics has a broad impact on determining the shear elasticity and viscosity of PNCs. Even though extensive investigations have been done to explore chain dynamics inside PNCs, widely different and often conflicting results are reported. On the small scale of local chain dynamics, both experimental and computational results demonstrated that a mobility gradient existed in the direction of NPs [1–3]. On the other hand, the NPs show no influence on local segmental dynamics of the chains adjacent to silica particles, compared with motions of the bulk chains [4].

More recently the dynamics of entangled polymer chains in PNC had been explored by neutron spin echo (NSE) experiments [5], from the initial Rouse dynamics to entanglement controlled motion, by filling hydrophobically modified (non-attractive) silica particles into a poly(ethylene-alt-propylene) (PEP) matrix. Authors reported several key findings: (i) the polymer behaves Gaussian even at high filler volume fractions, ϕ, (ii) the fillers are found to have no influence on the basic Rouse relaxation rate of PEP, (iii) the effective lateral confinement length or apparent tube diameter of PEP is decreasing with increasing ϕ, and (iv) a crossover from polymer chain entanglements to 'NP entanglements' (chain motion is hindered by NPs) is observed, with the critical ϕ_c determined to be 35% [5]. At the same time, both contour length fluctuation (CLF) and constraint release (CR) effects are suppressed by these NPs [6]. However, a rigorous link between the polymer chain dynamics and its entanglement status inside PNCs is still missing.

In this letter, we performed large scale isobaric molecular dynamics (MD) on a conventional finite-extensible non-linear elastic (FENE) spring model for polymer melts [7][I], filled by spherical non-attractive NPs of diameter D, with ϕ ranging from 0% to 42% (Fig. 1). Our normal mode analysis, primitive path (PP) and dynamic structure factor results on this simple model support the above key findings (i), (iii) and (iv). We find $\phi_c = 31\%$, exactly matching the percolation volume fraction of random spherical NPs in 3D [8]. While below ϕ_c, the normal mode relaxation can be accelerated by NPs due to the disentanglement behavior of polymer chains, adding NPs above ϕ_c slows down the relaxation processes. The basic Rouse relaxation rate is thus greatly affected by NPs. To our knowledge, the present study provides the first observation of disentanglement behavior within highly entangled polymer chains filled with NPs. Moreover, when $\phi < \phi_c$, the observed reduction of disentanglement time τ_d is linearly proportional to the reduction of entanglements per chain $\langle Z_{\mathrm{kink}} \rangle$ or tube diameter $\langle a_{\mathrm{pp}} \rangle^{-2}$, in agreement with the tube theory [9] which also indicates the polymer chain entanglement-dominated regime. However, if $\phi > \phi_c$, such a relationship will be broken down, due to the 'NP entanglements'.

High molecular weight polymers interpenetrate each other in melts; their dynamical behavior is controlled by quasi-topological constraints: chain connectivity and uncrossability. The constraints (entanglements) are commonly assumed to be able to effectively restrict the lateral motion of individual polymer chains to a tube-like region. Within this picture polymer chain travels back and forth, i.e. reptate, along the centerline of the tube-like region, defined as primitive path (PP). By applying the Z1 code [10, 11] on our fully equilibrated systems, we obtain the PP of chains inside PNCs under both the 'phantom' or 'frozen' particle limits [7][II]. The obtained mean PP length $\langle L_{\mathrm{pp}} \rangle$, tube diameter $\langle a_{\mathrm{pp}} \rangle$ as well as the entanglement number per chain $\langle Z_{\mathrm{kink}} \rangle$ under the 'phantom particle limit' are listed in Tab. I.

Upon increasing ϕ from 0% to 42%, the chains gradually disentangle; $\langle Z_{\mathrm{kink}} \rangle$ decreases from 10.07 down to 6.25. Snapshots of our PNCs and conformational analysis including the anisotropy of the tensor of gyration [7][I] supports the picture of gradually isolating chains, where an increasing amount of NP surface area helps stretching the chains
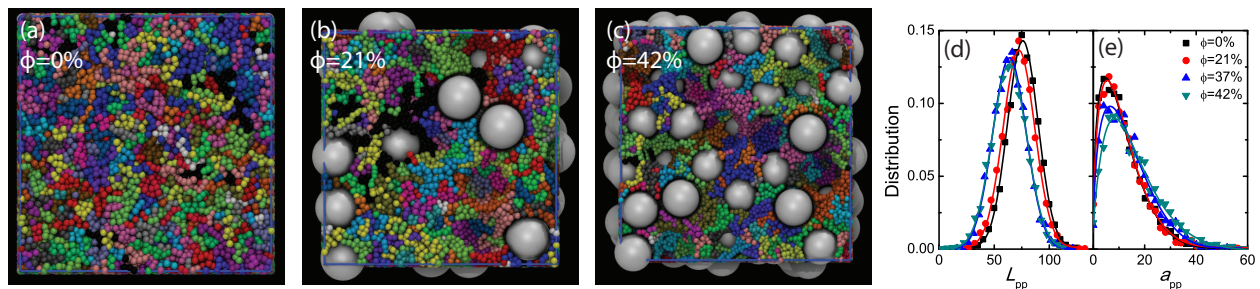
FIG. 1: (a)-(c) Snapshots of simulated systems at three different volume NP concentrations. Each chain has a randomly selected color, including black. NP effect on the distributions of (d) PP length L_{pp} and (e) tube diameter a_{pp}. Solid lines in (d) and (e) are fitted Gaussian and beta functions, respectively.

[12]. The observed disentanglement is in qualitative agreement with behavior reported for polymer chains inside cylindrical nanopores [13]. With the FENE chains disentangled, $\langle L_{pp}\rangle$ and $\langle a_{pp}\rangle$ are reduced and enlarged, respectively, as shown in Tab. I. The distributions of L_{pp} and a_{pp} generating these averages are given in Fig. 1. The two types of distributions can be well fitted by Gaussian and beta functions, respectively, indicating that the chains still preserve Gaussian conformations at high ϕ. Within the tube model [14], the τ_d is known to be proportional to $\langle Z_{kink}\rangle$ or $\langle a_{pp}\rangle^{-2}$ [9]. If we ignore additional mechanisms accompanying geometrical confinement induced by NPs, the dynamics of chains should thus get accelerated with increasing ϕ, since their $\langle Z_{kink}\rangle$ values are below the ones we find in the bulk. However, the geometrical effect of NPs plays an important role, when $\phi > 31\%$. We set out to demonstrate, that the dynamics of FENE chains is accelerated up to a critical concentration, due to a reduction of $\langle Z_{kink}\rangle$, and subsequently slowed down due to geometrical confinement.

The measured normal mode correlation functions of polymer chains at different ϕ we can capture by a stretched exponential, leaving us with a set of relaxation times τ_p^* and stretching parameters β_p (Fig. 2a). The fits do well in describing the data and get strongly non–exponential for modes $3 < p < 12$, as the β_p is away from unity (see [7]$_{IV}$). The stretching is expected since our polymer chains, as we already know from the PP analysis, are well-entangled. It is interesting to see that the first and second modes at $\phi = 31\%$ decays faster than that for both the $\phi = 0\%$ and 37% systems, indicating the dynamics of chains that firstly accelerates, and later slows down with increasing ϕ. When ϕ is very large, $\phi = 42\%$, the dynamics of chains are completely dominated by NPs: all the modes are slowed down. The τ_p^* with $p = 20$ for filler systems with $\phi = 42\%$ is about 58% larger than that of the unfilled system, which signifies extremely strong geometrical confinement due to the NPs. β_p, however, seems to be remain unaffected by ϕ, because our polymer chains basically exhibit Gaussian conformational statistics at all ϕ. The data more or less collapse onto the same curve. At the smallest length scales (large p values), $\beta_p \approx 0.7$, followed by a minimum of height 0.5 at around $N/p \approx 55$, and a further

increases to ≈ 0.8 at the largest scale ($p = 1$). Although the chains gradually disentangle during NP–filling (Tab. I), it is astonishing to see that all PNCs share the location of their minimum at $N/p \approx 55$, which is in value comparable to the entanglement length $N_e \approx 50$ for the unfilled system [17].

The short time decay behavior of the highest modes ($p = 20$) provides us with a bead friction coefficient ζ, the relaxation rate W [7]$_{IV}$, and the Rouse time τ_R (Tab. I). For the unfilled systems we find $\zeta = 25 \pm 0.54$, well in accord with the obtained value (25 ± 2) for $N > 100$ [16]. If $\phi < 10\%$, the NP effect on ζ is negligible. For $\phi \geq 20\%$, we observe an increment of ζ, i.e. $27 \sim 32$ as ϕ increases from 20% to 42% [7]. As noted already, the chains are stretched, isolated and disentangled [7], but geometrically hindered by NPs, when ϕ is very large. Therefore, ζ can be gradually increased upon filling. As a result, the Rouse time τ_R uprises with ϕ, contrary to the experimental finding of Schneider et al. [5], who did not observe a general slowing down of the basic Rouse modes.

Following the discussion of Padding and Briels [18], the disentanglement time τ_d we estimate from the long time asymptotic behavior of the first normal mode ($p = 1$). At time $t = \tau_d$, the first normal mode should have decayed to $1/e$ of its original value at $t = 0$ [18](see [7]$_{IV}$). Since our longest chain length is only about 8∼10 times of the entanglement length N_e, the obtained τ_d should be very close to the real disentanglement time, as discussed by Padding and Briels [18]. From the fitted results (Fig. 2a), we thus have direct access to the variation of τ_d with ϕ (Tab. I). Below $\phi = 31\%$, τ_d monotonically decreases with increasing ϕ. However, above $\phi = 31\%$, τ_d is suddenly much larger than that of pure chains ($\phi = 0\%$), and up to about 60% larger at $\phi = 42\%$. Clearly, the normal modes of polymers can be affected by the NPs, which appears unexpected in view of Schneider et al. [5], but is in accord with previous MD simulation results [19]. It had been established that the attractive polymer–NP interactions slow the relaxation, while the non-attractive polymer–NP interactions give rise to an increased rate of relaxation [20, 21]. These observations receive an interpretation through our findings on the τ_d of chains inside their PNCs ($\phi < 31\%$).

The effect of NP concentration on $\langle Z_{kink}\rangle$, τ_d, and their relationship is highlighted by Fig. 2b. It is interesting to see that

ϕ	M	M_{NP}	L	$\langle R_{ee}^2 \rangle^{1/2}$	$\langle R_g^2 \rangle^{1/2}$	W	ζ	$\tau_R/10^4$	$\tau_d/10^4$	$\langle L_{pp} \rangle$	$\langle a_{pp} \rangle$	$\langle Z_{kink} \rangle$
0%	212	0	50.0	$29.280^{a,b}$	11.856^a	0.071	25	35.71	261.58	72.612^b	11.866^b	10.065^b
5%	195	12	49.9	28.946	11.884	0.072	25	35.09	272.43	72.721	11.499	9.993
10%	178	24	49.8	29.004	11.928	0.072	25	35.09	244.53	70.269	11.942	9.467
21%	144	48	49.5	29.292	12.040	0.066	27	38.46	236.93	69.147	12.456	8.922
31%	110	72	49.3	28.921	11.786	0.056	32	45.53	199.56	63.932	13.088	7.632
37%	93	84	49.2	29.737	12.162	0.056	30	45.39	321.12	61.942	14.262	6.987
42%	132	165	58.8	31.372	12.648	0.051	30	49.23	430.53	61.535	16.003	6.252

TABLE I: Simulated systems. Volume fraction ϕ of NPs of diameter $D = 10$, number of polymer chains, M, number of NPs, M_{NP}, simulation box size, L. Results obtained for end-to-end distance, $\langle R_{ee}^2 \rangle^{1/2}$, radius of gyration, $\langle R_g^2 \rangle^{1/2}$, relaxation rate, W, bead friction coefficient, ζ, Rouse time, τ_R, disentanglement time, τ_d, PP length, $\langle L_{pp} \rangle$, tube diameter, $\langle a_{pp} \rangle \equiv d_{tube}$, number of entanglements per chain, $\langle Z_{kink} \rangle$. All the FENE chains have the length $N = 500$ and the polymer bulk number density is constant at 0.85 [7]$_I$. All quantities given in reduced LJ units. The tube diameter is $\langle a_{pp} \rangle = \langle R_{ee}^2 \rangle / \langle L_{pp} \rangle$ [15]. $\langle L_{pp} \rangle$, $\langle a_{pp} \rangle$ and $\langle Z_{kink} \rangle$ are obtained from the 'phantom particle limit'. See [7]$_{III}$ for the details. ^{a,b} Results for pure melts ($\phi = 0\%$) confirm previous works [16, 17].
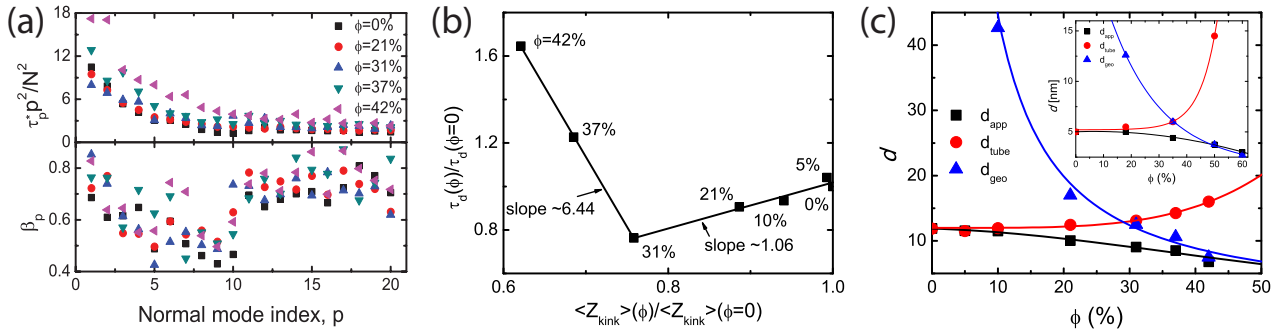

FIG. 2: (a) Normal mode analysis [7]$_{IV}$ results for (top) reduced relaxation times $\tau_p^* p^2 / N^2$ and (bottom) stretching parameters β_p corresponding to the first twenty modes of FENE chains with different NP volume fractions ϕ. (b) Reduced disentanglement time τ_d vs. reduced number of entanglements per chain $\langle Z_{kink} \rangle$ for PNCs with different ϕ. Below $\phi_c = 31\%$, the τ_d is found to be linearly proportional to $\langle Z_{kink} \rangle$, which indicates the 'polymer entanglements'-dominated regime [9]. Beyond $\phi_c = 31\%$, the $\langle Z_{kink} \rangle$ continues diminishing while τ_d increases with ϕ, characterizing the 'NP entanglements'-dominated regime. (c) Characteristic confinement length of FENE chains vs. ϕ, compared with experimental results for PEP polymers (inset, from Ref. [5]). d_{app} is the phenomenological/apparent tube diameter from $S(q,t)$/NSE measurements. d_{geo} is the calculated geometrical confinement length. d_{tube} is the topological tube confinement, or the tube diameter $\langle a_{pp} \rangle$ obtained from PP analysis. The solid lines guide the eyes.

the linear relationship between $\langle Z_{kink} \rangle$ and τ_d holds for relative amounts [9], when $\phi < \phi_c$; while, such a relationship will break down for $\phi > \phi_c$, due to 'NP entanglements'. Inline with the $\langle Z_{kink} \rangle$ behavior, we also find that $\tau_d \propto \langle a_{pp} \rangle^{-2}$ for the reduced quantities when $\phi < \phi_c$ (results not shown). With PP analysis and normal model results at hand, we can conclude that there is a crossover around $\phi_c = 31\%$, which indicates the transformation from chain entanglements to 'NP entanglements'. To be discussed in the following part, the NPs are very small and cannot contribute to an entanglement mesh of polymer chains. That is the reason why $\tau_d \propto \langle Z_{kink} \rangle$ when $\langle Z_{kink} \rangle$ is given by the 'phantom particle limit'.

Based on a mean field approach, Schneider *et al.* [5] developed a simple relationship $1/d_{app}^\nu(\phi) = 1/d_{tube}^\nu(\phi) + 1/d_{geo}^\nu(\phi)$ with exponent $\nu = 2$, where $d_{tube} \equiv \langle a_{pp} \rangle$ is the topological tube diameter as given in Tab. I; d_{geo} is the calculated geometrical confinement length (see [7]$_{III}$). A phenomenological 'apparent' tube diameter d_{app} can be obtained

through the NSE experiments or the coherent single chain dynamic structure factor $S(q,t)$ [7]$_V$. With the values of d_{app}, d_{tube} and d_{geo} at hand, the crossover from chain entanglements to 'NP entanglements' for PEP chains with silica NPs can be determined to be around 35% (inset of Fig. 2c). While d_{app} decreases, d_{tube} increases with increasing ϕ, inline with the proposed crossover from chain entanglements to 'NP entanglements' [5].

In PNCs, there are two important factors constraining the motion of polymer chains: one is the topological constraints or entanglements, which is reflected by the $\langle a_{pp} \rangle$ or $\langle Z_{kink} \rangle$ as shown in Tab. I; the other is the geometrical confinement length induced by NPs, which can be understood through the void distance distribution function of these NPs [5]. We evaluated this distribution [7]$_{III}$. With ϕ increasing from 21% to 42%, the void distance between two NPs dramatically decreases from 6.26 to 2.87. As a result, the dynamics of chains at $\phi = 42\%$ is tremendously slowed down (Fig. 2b). At the

highest ϕ, the void distance is roughly half of d_{app} (6.78), indicating that the chains are not completely hindered in their motion. Cai *et al.* [22] have studied the mobility of non-sticky NPs in polymer liquids. They found that NPs can diffuse more rapidly than polymer chains, when the NP size is small compared with d_{tube} of bulk polymer chains [22]. In our case, the NP diameter is $10 < d_{tube} \approx 12$ for the pure system. Therefore, the NPs move quickly, cannot contribute to an entanglement mesh and assist the anormal diffusion of chains at high ϕ (see [7]$_{IV}$). That is also the reason why we observe a large value of d_{app} at 42%. Yamamoto and Schweizer [23] recently elaborated on this phenomenon using a statistical dynamical theory, which also supplies a good explanation for the violation of the hydrodynamic Stokes–Einstein diffusion law for a spherical NP in entangled polymer melts. In the experiments of Schneider *et al.*, the NP diameter is about 17.0 ± 0.2nm, i.e., much larger than the tube diameter of PEP polymers ($\sim$ 5nm) [5]. For this case, the NPs are trapped by PEP entanglements and they can only move further by waiting for the PEP chains to relax by means of reptation [22, 23]. Thus, the apparent tube diameter should be completely determined by the void distance of hydrophobic silica NPs at the high $\phi = 50 \sim 60\%$ [5], cf. inset of Fig. 2c.

As we have calculated d_{tube} and d_{app} independently via PP analysis and $S(q, t)$, respectively, we can obtain d_{geo} via the relationship quoted above (see Fig. 2c). It is interesting to see that the calculated d_{geo} is about $2.6\times$ the corresponding analytical expression obtained by Torquato *et al.* [7, 24]. We speculate that this discrepancy is caused by the CLF and CR effects induced by the relatively small sizes of NPs considered in this letter. Both d_{app} and d_{geo} had been measured [5] from NSE and void distance distributions, respectively. With these two d's at hand, the third, d_{tube}, is evaluated based on the same relationship (inset Fig. 2c). Our simulation results agree surprisingly well with the experimental results (Fig. 2c). Our critical $\phi_c \approx 31\%$ seems to be in well accord with the $\phi_c \approx 35\%$ reported in [5].

It seems worthwhile emphasizing that we are not in a position proving the simple relationship between d_{app}, d_{tube} and d_{geo}, given by Schneider *et al.* [5]. As already noted elsewhere [6], the results from their mean field picture have limited validity, since $D \approx (2 - 3)\,d_{tube}\,(\phi = 0)$, which indicates CLF and CR effects being suppressed by the NPs. However, in our work, $D \approx d_{tube}\,(\phi = 0)$, which indicates NPs can diffuse much faster than that predicted by Stokes–Einstein diffusion law [23]. We had to multiply the calculated d_{geo} values by 2.6 to match this simple relationship. However, with this picture at hand, the critical NP volume fraction can be easily determined to be 31%, marking the transition from polymer to NP entanglements. Such a critical volume fraction also agrees reasonably well with our previous PP and normal model analysis results. The overall situation does not improve further if a exponent $\nu = 4$ is considered, a relationship proposed by Mergell and Everaers [25] upon considering that entanglements and geometrical confinements are represented by two sets of harmonic springs.

Tuteja *et al.* [26] have studied the rheological properties of linear entangled polystyrene (PS) filled with PS–NPs. They found that the zero-rate shear viscosity of such PNCs can be reduced by filling (up to $\phi \leq 20\%$) [26], in contrary to the traditional Einstein relation. They hypothesized that the PS–NPs can diffuse much faster than polymer chains, causing the CR effect to dominate. In this letter, we find that the chains gradually disentangle upon filling (Tab. I) and confirmed the faster diffusion behaviors of NPs. As long as $\phi < \phi_c$, geometrical confinement is negligible (Fig. 2c). Thus, the relaxation dynamics of chains is accelerated upon filling (up to ϕ_c), as demonstrated in Fig. 2a. As a direct consequence, the shear viscosity (inverse relaxation frequency) of our PNCs should decrease upon filling, as long as $\phi < \phi_c$. Our findings thus furthermore suggest a refined and microscopically supported view on how to explain the viscosity-reduction behaviors of PNCs, observed by Tuteja *et al.* [26].

* Corresponding author: w-liu@northwestern.edu
[1] H. Montes, F. Lequeux, and J. Berriot, Macromolecules **36**, 8107 (2003).
[2] A. Papon, K. Saalwachter, K. Schaler, L. Guy, F. Lequeux, and H. Montes, Macromolecules **44**, 913 (2011).
[3] F. W. Starr, T. B. Schroder, and S. C. Glotzer, Macromolecules **35**, 4481 (2002).
[4] R. B. Bogoslovov, C. M. Roland, A. R. Ellis, A. M. Randall, and C. G. Robertson, Macromolecules **41**, 1289 (2008).
[5] G. J. Schneider, K. Nusser, L. Willner, P. Falus, and D. Richter, Macromolecules **44**, 5857 (2011).
[6] K. Nusser, G. J. Schneider, and D. Richter, Soft Matter **7**, 7988 (2011).
[7] See section no. (specified by roman subscript) within the supplementary material EPAPS document ... .
[8] M. Powell, Phys. Rev. B **20**, 4194 (1979).
[9] The tube model [14] implies $\tau_d(\phi) \sim Z^2(\phi)a^2(\phi)N$. As long as $R_{ee}^2 = Z(\phi)a^2(\phi)$ is insensitive to ϕ (cf. Tab. I), $\tau_d(\phi)/\tau_d(\phi = 0) = Z(\phi)/Z(0) = a^2(0)/a^2(\phi)$.
[10] M. Kröger, Comput. Phys. Commun. **168**, 209 (2005).
[11] S. Shanbhag and M. Kröger, Macromolecules **40**, 2897 (2007).
[12] Y. Li, M. Kröger, and W. K. Liu, Macromolecules **45**, 2099 (2012).
[13] J. Martin, M. Krutyeva, M. Monkenbusch, A. Arbe, and al.,

Phys. Rev. Lett. **104**, 197801 (2010).

[14] M. Doi and S. Edwards, *The Theory of Polymer Dynamics* (Oxford, Clarendon, 1986).

[15] C. Tzoumanekas, F. Lahmar, B. Rousseau, and D. N. Theodorou, Macromolecules **42**, 7474 (2009).

[16] K. Kremer and G. S. Grest, J. Chem. Phys. **92**, 5057 (1990).

[17] R. S. Hoy, K. Foteinopoulou, and M. Kröger, Phys. Rev. E **80**, 031803 (2009).

[18] J. T. Padding and W. J. Briels, J. Chem. Phys. **117**, 925 (2002).

[19] R. Picu and A. Rakshit, J. Chem. Phys. **126**, 144909 (2007).

[20] C. J. Ellison and J. M. Torkelson, Nat. Mater. **2**, 695 (2003).

[21] F. W. Starr and J. F. Douglas, Phys. Rev. Lett. **106**, 115702 (2011).

[22] L. H. Cai, S. Panyukov, and M. Rubinstein, Macromolecules **44**, 7853 (2011).

[23] U. Yamamoto and K. Schweizer, J. Chem. Phys. **135**, 224902 (2011).

[24] S. Torquato, B. Lu, and J. Rubinstein, Phys. Rev. A **41**, 2059 (1990).

[25] B. Mergell and R. Everaers, Macromolecules **34**, 5675 (2001).

[26] A. Tuteja, M. E. Mackay, C. J. Hawker, and B. Van Horn, Macromolecules **38**, 8000 (2005).